Biochemical Pharmacology 81 (2011) 478–487

Contents lists available at ScienceDirect

Biochemical Pharmacology

journal homepage: www.elsevier.com/locate/biochempharm

Synergistic antimicrotubule therapy for prostate cancer

Vaishali Pannu, Prasanthi Karna, Hari Krishna Sajja, Deep Shukla, Ritu Aneja *

Department of Biology, P.O. Box 4010, Georgia State University, Atlanta, GA 30303, United States

ARTICLE INFO

Article history:
Received 23 August 2010
Accepted 5 November 2010
Available online 16 November 2010

Key words:
Tubulin-binding
Synergy
Polyploidy
Apoptosis
Docetaxel

ABSTRACT

Prostate cancer has been widely viewed as a chemoresistant neoplasm. Perhaps, the most prevalent antimicrotubule strategy involves docetaxel administration at its maximum-tolerated dose (MTD). Although the goal is to obtain total eradication of cancer cells, debilitating toxicities are presented by docetaxel therapy, including myelosuppression, immunosuppression, gastrointestinal toxicity and peripheral neuropathy. In addition, solubility limitations necessitate infusion of high-doses intravenously once or twice a week followed by a rest period, which allows recovery of normal proliferating cells to counter-balance efficacy. An emerging notion is that more of a toxic drug at its MTD is not necessarily better. It is likely that combinatorial antimicrotubule therapy with drugs occupying different sites on tubulin may enhance efficacy while reducing toxicity. Here we show that bromonoscapine (EM011), a microtubule-modulating noscapine analog, displays synergism with docetaxel as seen by cell viability and proliferation assays. Cell-cycle data demonstrated that lower dose-levels of docetaxel (25 nM) in combination with EM011 caused an additive increase in proapoptotic activity. Since docetaxel alone caused severe mitotic arrest followed by mitotic slippage and endoreduplication, we strategized a sequential treatment regime that involved initial pretreatment with docetaxel followed by addition of EM011 to maximize mitotic arrest and subsequent apoptosis. *In vivo* studies with docetaxel and EM011 in combination showed a marked inhibition of tumor growth compared to docetaxel or EM011 as single-agents. Our studies suggest the potential usefulness of EM011 in the clinic to enhance docetaxel activity. This would reduce toxicity, thus improving the quality of life of docetaxel-treated patients.

1. Introduction

Prostate cancer is the most common cancer among US men and a leading cause of mortality worldwide [1]. An overwhelming majority (~90%) of prostate cancer deaths occur in patients with skeletal metastases, particularly in bones [2]. Unfortunately, androgen-ablative therapy as first-line chemotherapy is only palliative, as tumors develop resistance to anti-androgens within 6 months to 2 years [3–6]. More recently, studies of docetaxel (taxotere) based chemotherapy have indicated significant survival benefits in this disease state in men with androgen-independent prostate cancer [7,8]. Since the most prevalent strategy involves docetaxel administration usually at its maximum-tolerated dose (MTD), debilitating toxicities are presented by docetaxel therapy including myelosuppression, immunosuppression, gastrointestinal toxicity, and peripheral neuropathy [9–14].

Systemic toxicity constitutes one of the major clinical impediments to successful chemotherapy. Much of this is attributable to the traditional usage of drugs at MTDs in the clinic. Solubility limitations of several drugs also necessitate infusion of high-doses intravenously once or twice a week, followed by a rest period, which unfortunately allows recovery of normal proliferating cells to counterbalance efficacy. This high-dosage strategy has also been popular perhaps due to limitations of non-specificity of drugs, wherein MTD would yield higher dose–response curves necessary for the management of patients in the terminal stages of cancer. However, treatment strategies involving MTD unfavorably result in a narrow therapeutic window with high-doses being toxic to rapidly proliferating normal cells of the body. An emerging notion is that more of a toxic drug at its MTD is not necessarily better. Recently, the idea of employing 'biologically effective doses' of a combination of one or more tubulin-binding drugs, that occupy different sites on tubulin, has gained momentum [15]. Essentially, the lower biologically effective doses of each drug would perhaps elicit a pharmacological response without causing overt toxicity. In addition, the use of lower biologically effective doses of a drug might confer an advantage of administering the drugs more often and may counteract off-target toxicities. This may also combat drug resistance encountered on using MTD. Most often, chemotherapy involves coadministration of two or more drug regimes in

* Corresponding author at: Department of Biology, Georgia State University, 100 Piedmont Ave, Atlanta, GA 30303, United States. Tel.: +1 404 413 5417.
E-mail addresses: vaishali.gsu@gmail.com (V. Pannu), karna14@yahoo.com (P. Karna), krishna70@yahoo.com (H.K. Sajja), deeprshukla@gmail.com (D. Shukla), raneja@gsu.edu (R. Aneja).

0006-2952/$ – see front matter © 2010 Elsevier Inc. All rights reserved.
doi:10.1016/j.bcp.2010.11.006

combination and several antimicrotubule drugs that bind at different sites on the same cellular target, for example tubulin, have been shown to display synergy in offering therapeutic responses [16–18]. This presents a unique opportunity to administer drugs at far lower concentrations than doses at which they individually exert toxicity. In addition, this enables lowering the concentration of more toxic drug while supplementing it with a more tolerable, less toxic drug.

Noscapine, a naturally occurring non-toxic plant alkaloid with known antitussive function has been identified for its novel tubulin-binding anticancer property [19]. Continued efforts directed towards rational drug design and chemical synthesis have yielded several potent noscapine analogs with superior pharmacologic and toxicity profiles [20–23]. One of them, EM011 (the brominated noscapine analog) has shown significantly higher activity than the parent noscapine, while retaining its non-toxic attributes [23–25]. Here we show that EM011 displays synergy with docetaxel in inhibiting cellular proliferation and inducing apoptosis in human prostate cancer cells. In view of the favorable toxicity profile of EM011, the synergism between EM011 and docetaxel *in vivo* offers a clinically relevant opportunity to utilize reduced dose-levels of docetaxel well below its MTD while combining it with daily oral EM011 doses for the chemotherapeutic management of prostate cancer. Such synergistic regimens perhaps will enable us to switch to a 'metronomic style of chemotherapy' where the tumor is never allowed to 'recover' by chronic administration of low doses of cytotoxic drugs in combination with more tolerable drugs at close, regular intervals with no prolonged drug-free interruptions.

2. Materials and methods

2.1. Cell culture and treatment schedule

PC-3 and DU145 cells were grown in RPMI medium supplemented with 10% fetal bovine serum (FBS) and 1% penicillin/streptomycin. For sequential combination treatment to strategize most effective outcome, treatment with 10 μM EM011 was performed for 12 or 24 h post 25 nM docetaxel treatment. The cells were then fixed for cell cycle analysis at 48 h post docetaxel treatment.

2.2. Cell viability by trypan blue-exclusion assay

The loss of membrane integrity in dead and dying cells allows preferential uptake of labels like trypan blue. At the end of incubation times with drugs, PC-3 cells were pelleted and washed with PBS. Well-suspended cells were mixed with equal volume of 0.4% trypan blue in 1× PBS, pH 7.4, followed by incubation at room temperature for 5 min. Cells were examined under the microscope and blue-stained cells were considered non-viable.

2.3. Alamar blue assay

Growth inhibition of cells was measured using the Alamar blue assay. This assay is an indicator of the ability of metabolically active cells to reduce non-fluorescent resazurin to bright red-fluorescent resorufin. Briefly, cells were plated at 10^4 cells/well in a 96-well plate-format. After incubation with drugs, 20 μl of Alamar blue dye was added to each well, followed by incubation at 37 °C for 2 h and reading at 575 nm.

2.4. Determination of synergy and DRI

Drug interactions were analyzed by a computer software, Calcusyn, in a stepwise fashion, beginning with single agent dose–response curves, followed by dose–response curves involving combinations of the two drugs. The analytical method of Chou and Talalay [26] yields two parameters that describe the interactions in a given combination: the combination index (CI) and the dose reduction index (DRI). The combination index (CI) equation is based on the multiple drug-effect equation of Chou–Talalay derived from enzyme kinetic models. For mutually exclusive drugs that have the same or similar modes of action, combination index is described as $CI = (D)_1/(D_x)_1 + (D)_2/(D_x)_2$, where $(D_x)_1$ and $(D_x)_2$ are the doses of drug 1 and drug 2 alone, respectively, causing x% inhibition. A CI of <1 indicates synergism, a CI of 1 or close to 1 indicates additive effects, and a CI of >1 indicates antagonism. DRI measures the factor by which the dose of each drug in a combination may be reduced at a given effect level compared with the dose when each drug is used alone. DRI is important in clinical situations, where dose reduction leads to reduced toxicity while retaining the therapeutic efficacy. The dose-effect relationship was derived by Chou through mathematical induction using numerous enzyme kinetic models. It correlates the "Dose" and the "Effect" in the simplest possible form: $f_a/f_u = (D/D_m)^m$, where D is the dose of drug, and D_m is the median-effect dose signifying the potency. D_m is determined from the x-intercept of the median-effect plot. f_a is the fraction affected by the dose and f_u is the fraction unaffected ($f_u = 1 - f_a$). m is an exponent signifying the sigmoidicity (shape) of the dose effect curve. It is determined by the slope of the median effect plot. A DRI >1 is beneficial, and the greater the DRI value, the higher the dose reduction is for a given therapeutic effect. DRI may be influenced by the combination ratio and the number of drugs. Toxicity may be decreased when the dose is reduced.

2.5. DAPI staining

Cell morphology was evaluated by fluorescence microscopy following DAPI staining. PC-3 cells were grown on coverslips in six-well plates and were treated with drugs for 48 h. After incubation, coverslips were fixed in cold methanol and washed with PBS, stained with DAPI, and mounted on slides. Images were captured with Zeiss (Axioplan-2) fluorescence microscope using a 40× objective. Apoptotic cells were identified by features characteristic of apoptosis (e.g., nuclear condensation, formation of membrane blebs, and apoptotic bodies).

2.6. Immunoblotting

The protein lysates collected from control or treated cells were resolved by SDS-PAGE and transferred onto PVDF membrane. The membrane was incubated with the desired primary antibody overnight at 4 °C and appropriate secondary antibody for 1 h at room temperature. The immunoreactive bands were visualized by the chemiluminescence detection kit (Pierce Chemical Co., Rockford, IL). β-Actin was used as loading control.

2.7. Cell-cycle analysis

The flow-cytometric evaluation of cell-cycle status was performed using FlowJo software. After treatments, cells were harvested at different time intervals, washed twice with ice-cold PBS, and fixed in 70% ethanol for at least 24 h. Cell pellets were then washed with PBS followed by RNase A (2 mg/ml) addition and staining with anti-MPM-2 primary antibody and Alexa-488 conjugated secondary antibody. Propidium iodide (0.1% in 0.6% Triton X-100 in PBS) was added for 45 min in dark followed by analysis on a FACS Canto flow-cytometer (BD Canto).

2.8. Immunofluorescence microscopy

PC-3 cells were grown on glass coverslips for immunofluorescence microscopy. After treatment with drugs, cells were fixed with cold (−20 °C) methanol for 10 min and blocked by incubating with 2% BSA/PBS at 37 °C for 1 h. Cleaved caspase-3 or cleaved PARP antibodies (1:500 dilution) were incubated with the coverslips for 2 h at 37 °C. The cells were washed with 2% BSA/PBS for 10 min at room temperature before incubating with a 1:500 dilution of Alexa-488 conjugated secondary antibodies. Cells were mounted with Prolong-Gold antifade reagent that contained DAPI (Invitrogen, Carlsbad).

2.9. In vivo drug administration and tumor imaging

Stably-transfected luciferase-expressing PC-3 (PC-3-luc) cells (106) (Caliper Life Sciences, Alameda, CA) were subcutaneously injected in the right flank of six-week old male BALB/c nude mice (Harlan laboratories, IN). Growth of inoculated cells was monitored by measuring luciferase activity in live mice using the IVIS imaging system (Caliper Life Sciences, Alameda, CA) as described earlier [27]. Tumors were allowed to grow until measurable photon intensity and animals were then randomly subdivided into 4 groups of 5 mice each. Mice were fed daily with 300 mg/kg EM011 by oral gavage or 5 mg/kg docetaxel once a week intraperitoneally, or a combination of EM011 and docetaxel at dose levels used for single-drug treatments. Mice in control group received equal volume of vehicle (0.5% Tween-80 in PBS). All animal experiments were performed in compliance with the institutional IACUC guidelines. At the end of 5 week treatment, animals were sacrificed and tumors and other organs were excised for H&E and immunohistochemical staining as described earlier [27].

2.10. Statistical analysis

All experiments were repeated three times. Data were expressed as mean ± standard deviation. Statistical analysis was performed using Student's *t*-test. The criterion for statistical significance was $p < 0.05$. For immunoblotting data, band intensities were measured using ImageJ and normalized to β-actin.

3. Results

3.1. In silico docking of EM011 and docetaxel on tubulin

Both docetaxel and EM011 belong to the tubulin-binding family of chemotherapeutic agents [27–29]. Thus, we first asked if EM011 and docetaxel share the same binding site on tubulin. To this end, *in silico* molecular-modeling tools were employed to dock EM011 and docetaxel onto the 3.5 Å crystal structure of tubulin. Since the discovery of the anti-mitotic activity of the founding molecule, noscapine, was based on its structural similarities to known tubulin-binding drugs including colchicine [19], we used the solved structure of colchicine [30] as a basis to create an *in silico* model of EM011 bound to tubulin. Schrodinger's Phase Flexible Ligand Superpositioning program [31] was used to overlay the best-fitting conformation of EM011 onto colchicine, which was then placed into the pocket occupied by colchicine in the 1SA0 PDB structure [31,32]. We then used Matchmaker of UCSF's Chimera program [33,34] to align the β-subunit of our tubulin-EM011 model construct onto the corresponding β-subunit of the 1JFF PDB structure of tubulin complexed with docetaxel [35] to compare the relative binding locations of each drug, as shown in Fig. 1. Our molecular-modeling data revealed that EM011 docks onto β-tubulin at the interface with its dimerization partner, α-tubulin. Though both drugs share a common cellular target, they occupy different regions of the protein, suggesting that they can act synergistically. This could offer the therapeutic advantage of decreasing the dosage of docetaxel, the more toxic drug.

3.2. EM011 synergizes with docetaxel to decrease viability of PC-3 cells

Having identified that docetaxel and EM011 perhaps bind at different sites on tubulin based on our *in silico* model, we next wanted to examine if both drugs could effectively be employed together to produce synergistic effects. Essentially, a synergistic relationship would increase drug efficacy at lower dose-levels thus, reducing high-dosage toxicity and drug resistance. To this end, we evaluated the sensitivity of human prostate cancer PC-3 cells towards various combination regimens of docetaxel and EM011 using the trypan blue exclusion assay. The treatment strategy included five dose-levels of docetaxel (0.001, 0.005, 0.01, 0.05 and 0.1 μM) (Fig. 2Ai) and EM011 (0.1, 0.5, 1, 5 and 10 μM) (Fig. 2Aii) as single-agents or in various combinations (0.005, 0.01 or 0.05 μM docetaxel combined with 0.5 or 1 μM EM011) (Fig. 2Aiii). Cells were stained with trypan blue at 72 h after the specified treatments. The synergy upon treatment with EM011 and docetaxel was evaluated using the combination index (CI) method. The CI value of the combination of drugs was calculated using the Calcusyn software based on the isobolographic method. In essence, a CI equal to 1 characterized the interaction between the drugs as additive, whereas a CI > 1 and CI < 1 indicated an antagonistic and a synergistic relationship, respectively (Suppl. Table 1). Based on the percentage of cell death, the FA (fraction affected) upon each treatment was used to derive the corresponding CI values. Using the CI method, our results indicated a synergistic interaction between 0.05 μM docetaxel and 0.5 μM EM011 wherein the drug combination resulted in ~90% cell death (Fig. 2Aiii). This was significantly higher than treatment with each drug as a single-agent, in that we observed ~69% cell death with 0.05 μM docetaxel and ~10% cell death with 0.5 μM EM011 treatment.

Table 1 collates the fraction of cells affected and the CI values upon treatment with various combinations of docetaxel and EM011. Graphical representation of FA vs CI shows synergistic interaction between docetaxel (0.005 or 0.05 μM) and EM011 (0.5 or 1 μM) (Fig. 2Aiv). The calculated CI values corresponding to the specific combinations (Table 1A) indicated a strong synergistic interaction between 0.05 μM docetaxel and 1 μM EM011 (CI ~0.31). An equally comparable synergistic relationship was observed between 0.005 μM docetaxel and 1 μM EM011 (CI ~0.44). Interestingly an increase in concentration of docetaxel by 10-fold resulted in a mere ~3% increase in FA. Thus, it is suggested that 0.005 μM docetaxel and 1 μM EM011 may be a better therapeutic combination regimen as almost the same effect can be achieved with a 10-fold lower docetaxel dose-level. We also observed similar trends of enhanced cytotoxicity upon combination of docetaxel and EM011 in DU145, an androgen-independent PTEN-proficient prostate cancer cell line (Suppl. Fig. 2).

3.3. EM011 synergizes with docetaxel to cause growth inhibition of PC-3 cells

To further confirm synergy, we evaluated the antiproliferative potential of the drugs, docetaxel and EM011, as single-agents and in combination, using the Alamar blue assay. PC-3 cells were treated with docetaxel and EM011 individually and in combination for 72 h using concentrations shown in Table 1B. Since some of the drug combinations used earlier did not show significant synergy, we decided to include combinations (Table 1B) based on IC_{50} values of the two drugs. The IC_{50} of docetaxel and EM011 for PC-3

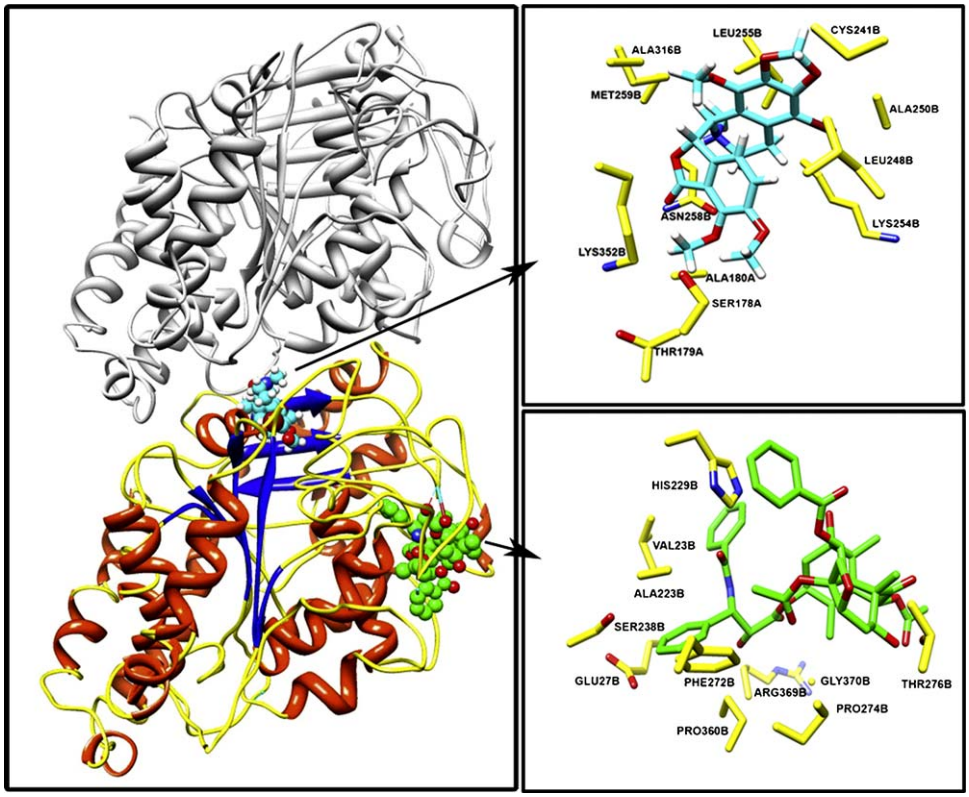

Fig. 1. *In silico* model construction of docetaxel (green) and EM011 (cyan) simultaneously bound to tubulin based on 1SA0 [30] and 1JFF [35] PDB structures. The α-tubulin subunit is shown in grey and the β-tubulin subunit in a colored secondary structure. EM011 is shown bound to β-tubulin at the solved binding site of colchicine near the intra-dimer intersection, distinct from that of docetaxel. The upper and lower panels on the right show zoom-in with the relevant amino acid residues in close proximity with docetaxel (lower, green) and EM011 (upper panel, cyan). (For interpretation of the references to color in this figure legend, the reader is referred to the web version of the article.)

cells were found to be 0.01 μM and 5 μM respectively (Fig. 2Ai and Aii). The drugs were used in combination at equipotent ratios, consistent with the ratio of their IC_{50} values (docetaxel:EM011=1:500). Interestingly, a synergistic interaction was observed for all the combinations studied (Table 1B). Fig. 2Bi depicts an increase in FA indicative of enhanced antiproliferative effect, upon cotreatment with increasing dose-levels of docetaxel and EM011 at a constant ratio. A plot of the fraction of affected cells vs CI indicates that docetaxel and EM011 showed strong synergy, as CI values at all combinations are below 1.0 (Fig. 2Bii). Maximum synergy, measured in terms of CI was observed using combination regimen of 5 or 7.5 nM docetaxel with 500-fold higher concentrations of EM011, with the CI values being 0.32 and 0.40, respectively (Table 1B). We next determined DRI, which is indicative of the magnitude by which a given drug dose can be reduced upon employing a combination regimen of two or more drugs compared to each drug as a single-agent. The DRI was ~4.5-fold higher for the most-effective combination of 5 nM docetaxel and 2.5 μM EM011 that yielded the lowest CI of ~0.321 indicating strong synergism between the two drugs. These data were encouraging and seemingly offer a unique opportunity to lower the dose-level of docetaxel by employing it in combination with EM011, a well-tolerated, relatively non-toxic drug [23–25,36].

3.4. EM011 enhanced docetaxel-induced nuclear fragmentation and apoptosis

Having identified the synergy between docetaxel and EM011 in reducing cellular viability and inhibiting cell proliferation, we next examined induction of cell death by evaluating nuclear morphology upon staining with a DNA dye, DAPI. PC-3 cells treated for 48 h with docetaxel (25 nM), EM011 (10 μM) and combination (25 nM docetaxel + 10 μM EM011) were fixed and stained with DAPI to examine the nuclear morphology in treated cells. Cells treated with the combination-dose showed the maximum number of fragmented nuclei (~80%), followed by docetaxel (~58%) and EM011 (~19%) (Fig. 2Ci and Cii). In addition, we also measured hypodiploid sub-G1 population with fragmented DNA, an indicator of apoptosis, by staining PC-3 cells with propidium iodide (PI), a DNA intercalating dye, using flow-cytometry (Fig. 2Di). In contrast to a low sub-G1 population with 25 nM docetaxel treatment (~54%) or 10 μM EM011 (~25%), the combination regimen (25 nM docetaxel + 10 μM EM011) resulted in a significant increase in sub-G1 population of ~82% (Fig. 2Dii). These data suggest an additive effect on sub-G1 population at 48 h upon cotreatment with docetaxel (25 nM) and EM011 (10 μM) (Fig. 2Di and Dii).

3.5. Sequential treatment resulted in synergistic apoptosis

Although we observed remarkable synergism in antiproliferative activity, our cell-cycle data with the most-effective combination regimen of docetaxel and EM011 mostly showed an additive effect on sub-G1 population. To explore this further and strategize enhancement of apoptosis, we closely examined the effect of the drugs as single-agents on the cell-cycle events over time. Since PI staining cannot distiguish between G2 and mitotic-phase populations (both have 4N DNA), MPM-2 antibody was used to stain for mitotic cells. Our results revealed that docetaxel at 25 nM caused a prolonged mitotic arrest between 12 and 24 h that peaked to ~38% (Fig. 3Ai and Aii). Subsequently, cells exited from mitosis as evident by loss of MPM-2 staining at 48 h (Fig. 3Aiii and Aiv). Our immunofluorescence confocal microscopy data was in concordance with the dual-color FACS data (Fig. 3Bi and Bii) and demonstrated the appearance of large multinucleated cells

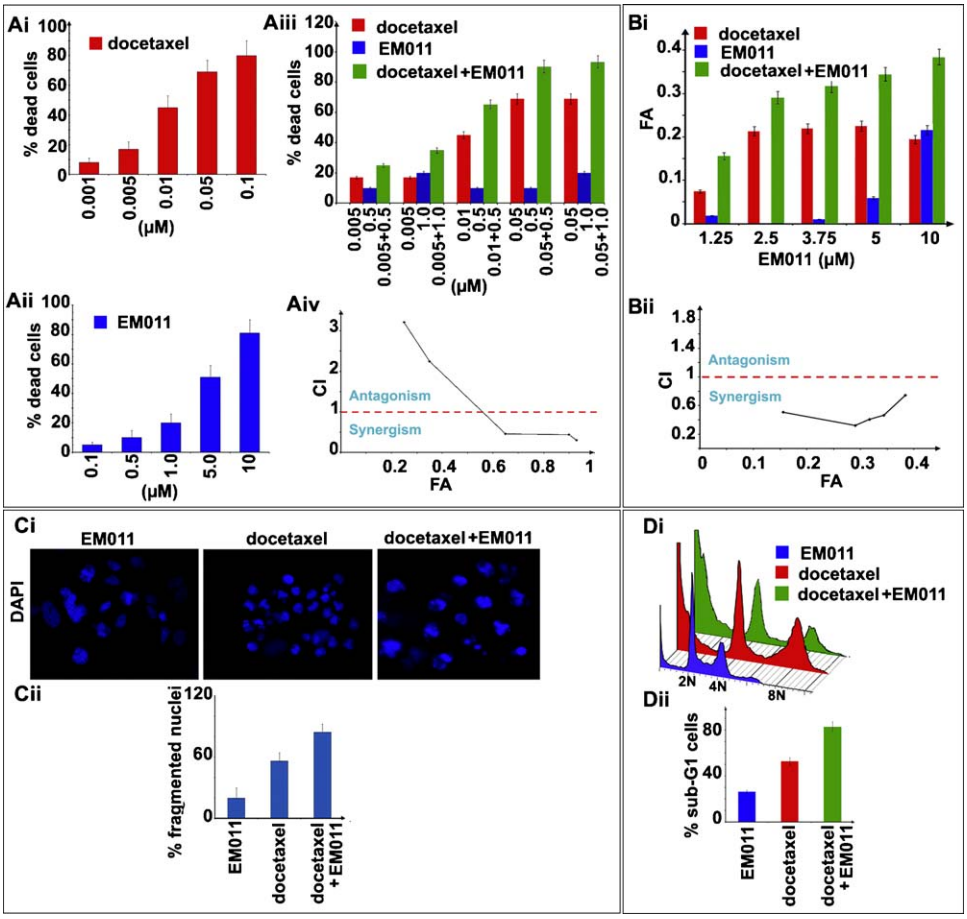

Fig. 2. (Ai) PC-3 cells were treated with varying dose-levels of docetaxel (0.001, 0.005, 0.01, 0.05, 0.1 μM), (Aii) EM011 (0.1, 0.5, 1, 5, 10 μM), (Aiii) docetaxel + EM011 at different concentrations for 72 h. The percentage of dead cells upon various treatments was measured using trypan blue staining. (Aiv) Line-graph of CI vs FA of PC-3 cells treated with various combinations of docetaxel and EM011 as shown in (Aiii). The red-dotted line indicates CI value of 1, below which drug combinations are considered to show synergistic effect. The degree of synergistic interactions was calculated using the Calcusyn software and quantitated in terms of CI. (Bi) Bar-graphical representation of fraction of cells affected (FA) by docetaxel and EM011 as single-agents as well as in combination as measured by Alamar blue assay. The concentration of EM011 is plotted on the *x*-axis and docetaxel concentration used at a fixed ratio (docetaxel:EM011, 1:500). (Bii) A line-plot of CI versus FA of PC-3 cells treated with the fixed ratios of EM011 and docetaxel shown in (Bi). The red-dotted line indicates CI value of 1, below which the combination of drugs are considered to show synergistic effect. (Ci) Fluorescence images (40×) of PC-3 cells stained with DAPI on treatement with docetaxel (25 nM), EM011 (10 μM) or combination (25 nM docetaxel + 10 μM EM011). (Cii) Quantitation of the percentage of fragmented nuclei resulting from the treatments. (Di) Cell-cycle overlays showing sub-G1 population of PC-3 cells treated with EM011 (10 μM), docetaxel (25 nM) and their combination (25 nM docetaxel + 10 μM EM011). (Dii) Bar-graphic representation of percent sub-G1 population analyzed by flow-cytometry. (For interpretation of the references to color in this figure legend, the reader is referred to the web version of the article.)

Table 1
(A) Different combination doses of docetaxel and EM011 indicating the resulting FA using trypan blue assay and the corresponding CI for the particular combinations used. (B) Different combination doses of docetaxel and EM011 in a fixed ratio of docetaxel:EM011 (1:500), indicating the resulting FA using Alamar blue assay and the corresponding CI for the particular combinations used.

(A) Cell viability (trypan blue assay)

EM011	Docetaxel	Combination	
Dose (μM)	Dose (μM)	FA	CI
0.5	0.005	0.25	3.21
0.5	0.01	0.35	2.25
0.5	0.05	0.65	0.46
1	0.005	0.90	0.44
1	0.05	0.93	0.31

(B) Cell proliferation (Alamar blue assay)

EM011		Docetaxel		Combination	
Dose (μM)	FA	Dose (μM)	FA	FA	CI
1.25	0.018	0.0025	0.0741	0.155973	0.51
2.5	0.0005	0.005	0.2129	0.290389	0.32
3.75	0.01	0.0075	0.2196	0.316972	0.40
5	0.0591	0.01	0.2251	0.343537	0.46
10	0.2158	0.02	0.1941	0.383859	0.74

indicating mitotic exit at 36 h of docetaxel treatment. The apoptotic population at 48 h was ~42% (Fig. 3Aiii). Interestingly, the mitotically exited cell population entered another round of cell-cycle as evident by the appearance of 8N mitotic population at 72 h of taxotere exposure (Fig. 3Aiv). Several reports suggest that absence of an intact p53 tetraploidy checkpoint can lead to endoreduplication of cells [37–39]. Thus, endoreduplication of PC-3 cells may be partially due to the absence of p53 in these cells [40]. In addition, mitotic arrest without subsequent apoptosis has been commonly observed following taxane treatment in various cancer cells [41]. Thus, failure to initiate apoptosis during or after mitotic arrest appears to be a major factor limiting the efficacy of antimitotic drugs. Furthermore, cancer cells can resist apoptosis by premature mitotic-exit, before cells initiate apoptosis, due to a weak mitotic checkpoint or rapid slippage out of mitosis [42]. Our data show that docetaxel-treated PC-3 cells undergo mitotic-exit at 36 h followed by endoreduplication. Recently, mitotic-slippage and apoptosis have been viewed as two competing pathways [43]. Consistent with the view that mitotic-exit protects cells from death, premature exit from mitotic arrest due to a weakened or ablated spindle assembly checkpoint has been shown to decrease sensitivity to spindle-perturbing drugs [42]. This notion has

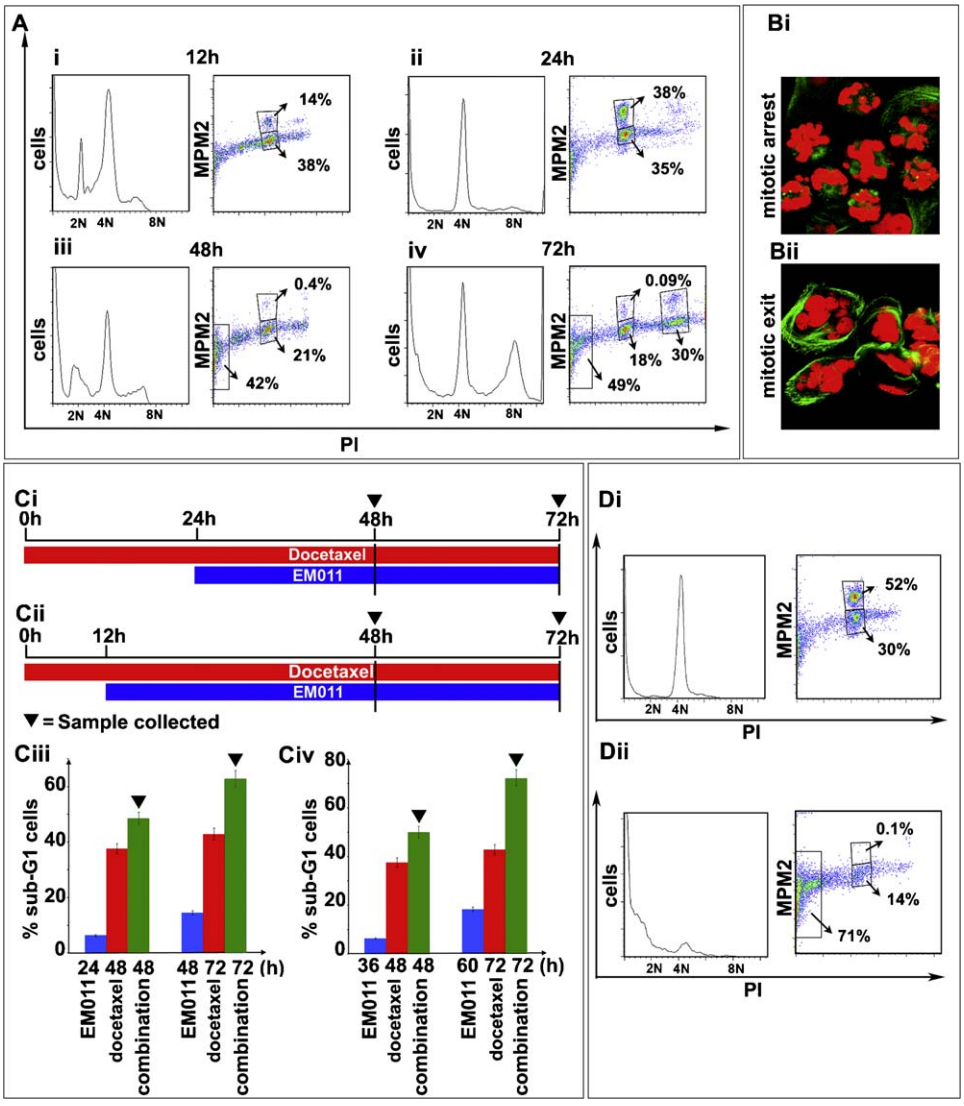

Fig. 3. (Ai–iv) Cell-cycle histograms of doubly-stained PC-3 cells treated with docetaxel at 25 nM concentration for 12, 24, 48 and 72 h showing mitotic arrest in (Ai) and (Aii), mitotic exit in (Aiii) and polyploid population in (Aiv), respectively. (Bi and ii). PC-3 cell0s treated with docetaxel (25 nM) for 24 h (Bi) and 48 h (Bii) and stained with α-tubulin (green) and DNA (red), indicating mitotic arrest (24 h, Bi) and polyploid population (72 h, Bii), respectively. (Ci and ii) Schematic representation of the sequential treatments performed on PC-3 cells. (Ciii and iv) Bar-graphs showing the percentage of sub-G1 population resulting from the sequential treatments (according to scheme Ci and Cii, respectively). (Di and ii) Cell-cycle histogram of PC-3 cells treated with docetaxel (25 nM) followed by EM011 (10 μM) after 12 h, and the cells were fixed at 36 and 60 h of EM011 treatment (scheme Cii). (For interpretation of the references to color in this figure legend, the reader is referred to the web version of the article.)

provided strong evidence to show that mitotic-exit is a promising therapeutic target, and that blocking mitotic-exit may be a better strategy for killing apoptosis-resistant, slippage-prone, cancer cells [42]. On similar lines of thought, we reasoned that timing the addition of EM011 which induces mitotic arrest as early as 6–8 h that peaks at 12–18 h, may prolong the duration and intensity of docetaxel-induced mitotic arrest. This may thus prevent cells from slipping out of mitosis and subsequent endoreduplication. To this end, we devised an experimental strategy wherein EM011 was added to PC-3 cells 12 and 24 h post docetaxel-treatment. Essentially, the rationale behind this treatment strategy was to produce a significant and extended mitotic arrest such that cells are chronically stalled in mitosis. The protracted mitotic arrest may not only reduce the chances of slipping out but may also result in the generation and accumulation of proapoptotic signals to maximize apoptotic responses [44]. It is also likely that sequential treatment may cause overlapping of maximally achievable intracellular concentrations of biologically effective doses of each drug to trigger robust apoptosis during the mitotic arrest. PC-3 cells were pretreated with 25 nM docetaxel for 12 or 24 h followed by treatment with 10 μM EM011 according to the schematic diagram (Fig. 3Ci and Cii). Cells were fixed for cell-cycle analysis at 48 and 72 h after docetaxel addition (Fig. 3Ciii and Civ). Flow-cytometric analysis of the samples from scheduled treatments showed an enhanced mitotic population (~52%) and a strong decrease in the polyploid (endoreduplicated) population (Fig. 3Di). There occurred a significant increase in sub-G1 population (~71%) at 72 h (Fig. 3Dii) (the scenario when EM011 was added 12 h after docetaxel treatment, Fig. 3Cii scheme), compared to when docetaxel was used as a single-agent (~49% sub-G1) (Fig. 3Aiv). Although a synergistic increase in the sub-G1 population (Fig. 3Ciii and Civ), indicative of apoptosis induction, was observed upon sequential drug treatment following both strategies, the magnitude of sub-G1 was higher when EM011 was added 12 h post docetaxel addition (Fig. 3Ci and Cii). Induction of apoptotic cell death was further confirmed by the presence of proapoptotic markers such as cleaved caspase-3 and PARP expression (Fig. 4). A synergistic increase in the expression of both activated caspase-3

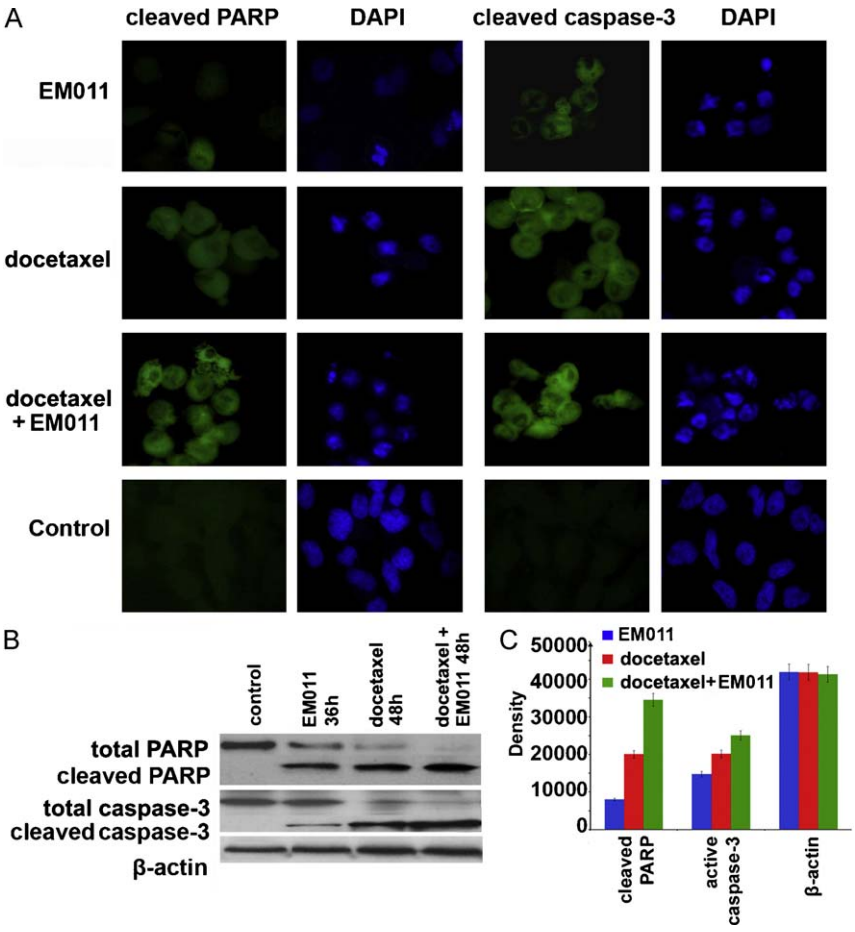

Fig. 4. (A) Immunofluorescence images of PC-3 cells treated with the docetaxel and EM011 schedule treatment (according to scheme Fig. 3Cii). Cells were pretreated with docetaxel for 12 h before addition of EM011 and were fixed at 48 h post docetaxel treatment compared to treatment with EM011 (10 μM for 36 h), or with docetaxel (25 nM for 48 h). Left panel shows cleaved PARP expression, whereas the right panel shows cleaved caspase-3 expression in PC-3 cells. (B) Immunoblot showing the expression of cleaved as well as total PARP and caspase-3 in PC-3 cells treated per the above mentioned schedule. β-Actin was used as a loading control. (C) Bar-graphs showing integrated density values representing the respective immunoblot that were normalized to β-actin. Quantitation of the band-intensity of immunoblots was done using ImageJ software.

and cleaved PARP was observed in cells treated according to scheme Fig. 3Ci, by immunofluorescence and western blot analysis (Fig. 4A and B). The immunoblot bands are quantified in Fig. 4C. The immunoblotting data correlated well with caspase activity in PC-3 cells using the same treatment regimes (Suppl. Fig. 2). These data suggested that in-depth analysis of temporal cell-cycle events and optimal timing of combination drug regimens can lead to development of synergistic drug combinations that can yield maximal therapeutic responses to improve disease-free survival.

3.6. EM011 and docetaxel synergistically inhibit in vivo tumor growth

After establishing the effective dose of docetaxel that can be used in combination, we investigated the effects of combining docetaxel and EM011 on tumor growth response in prostate tumor xenografts implanted in nude mice. To this end, we subcutaneously injected mice with PC-3, human androgen-independent prostate cancer cell line that stably expresses luciferase (PC-3-luc). It enabled visualization and monitoring of prostate cancer growth non-invasively in real-time [45]. The single-agent and combination drug schedule were designed to reflect a clinically relevant approach with docetaxel (5 mg/kg bw) administered intraperitoneally once a week and EM011 (300 mg/kg bw) fed by oral-gavage on a daily-basis. At the end of the 5 week treatment, vehicle-treated control mice (0.5% Tween-80) showed unrestricted tumor growth (Fig. 5A, Bi and Bii). Although single-agent drug regimes decreased tumor growth and progression compared to control, combination of docetaxel and EM011 caused a pronounced reduction in tumor volume as well as bioluminescent cell-counts compared with all other treatments (Fig. 5A, Bi and Bii). Quantitation of tumor volume revealed a reduction by ∼64% in docetaxel, ∼35% in EM011 and ∼89% in docetaxel + EM011 groups after 5 weeks of treatment, compared to control (Fig. 5Bii). In addition, insignificant reduction in the body weights of treated mice was observed over a period of 5 weeks, suggesting non-toxicity of combination treatment (Fig. 5Biii).

To elucidate *in vivo* molecular mechanism of drug treatments, immunostaining for cleaved caspase-3, cleaved PARP, TUNEL staining (apoptosis marker) and Ki67 (a marker for cell proliferation) was performed (Fig. 6A). We found ∼2-fold increase in TUNEL-positive cells in docetaxel + EM011 treated tumors compared to either treatment alone (Fig. 6A and Bi). Furthermore, there was a significantly high expression of cleaved caspase-3 and PARP in the combination group (∼2–3-fold, Fig. 6Bi). In addition, tumor samples from groups receiving combination therapy showed marked reduction in Ki67 positive cells compared with controls (Fig. 6A). Fig. 6Bii shows bar-graphical representation of Ki67 positive tumor cells for all treatment groups. The *in vivo* data thus offers strong evidence for the enhanced therapeutic benefits of combining docetaxel with EM011.

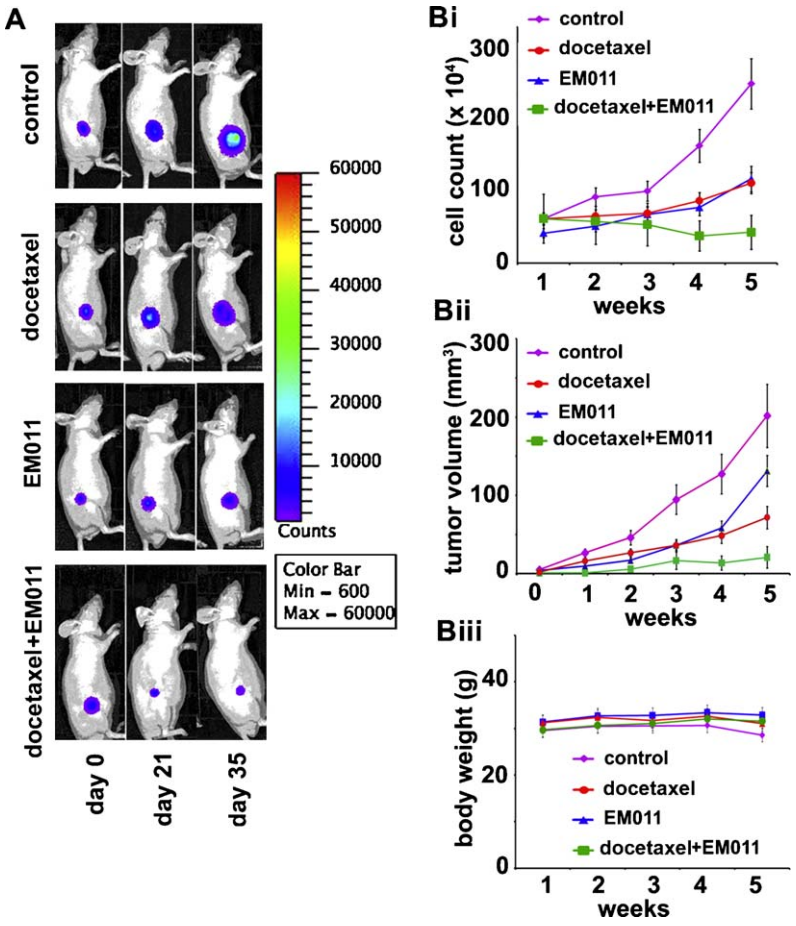

Fig. 5. (A) Representative bioluminescent imaging data from various treatment groups. (Bi) Quantitation of cell-counts from bioluminescent images. (Bii) Tumor volume measurements. (Biii) Body weight of mice from control, docetaxel, EM011 and combination of docetaxel and EM011 treated groups.

4. Discussion

Chemotherapy for advanced prostate cancer is a promising development, but carries the risk of undesirable side effects. Often, when considering treatment options, the real question is not only that the drugs improve survival, but do they improve survival enough to put up with greater toxicity? To alleviate toxicity, infrequent drug administration is opted that makes tumor elimination highly unlikely since the kinetics of tumor tissue recovery is much faster than that of normal tissue recovery. Since advanced hormone refractory prostate cancer is not yet curable, it is a disease patients may have to live with, often for many years, which puts a premium on quality of life.

Hormone refractory prostate cancer management using secondary hormonal manipulations, mitoxantrone-based chemotherapy, external beam radiation therapy, or radioisotope therapy has at best achieved palliation. Recently, docetaxel has been FDA-approved as the standard first-line therapy for patients with advanced prostate cancer that fail to respond to androgen ablative therapy. As shown by two randomized clinical trials in 2005, patient survival with docetaxel-based therapy improved by 20–24% when compared to survival with mitoxantrone and prednisone therapy [46]. Although currently-available chemotherapeutic regimens employing docetaxel for prostate cancer management cause significant transitory regression in tumor-cell numbers, a near-complete cure is rarely achieved. This is because intermittent dosing allows tumor regrowth between treatment schedules. At diagnosis, a clinically detectable solid tumor contains 10^9–10^{11} cells, all of which need to be killed to achieve a cure. Even if docetaxel therapy kills 90% or even 99.9% of tumor cells, the end result will still be only a temporary partial regression and a delay in the growth of the prostate tumor mass. Besides toxicity issues that impair the quality of life, the low aqueous solubility of docetaxel and the development of clinical drug resistance have led to a search for new drugs/combination regimens that show maximum therapeutic efficacies with diminished toxicity.

Since the paramount goal is to maximize benefit while minimizing toxicity, we sought to investigate drug combinations of docetaxel with agents that have a favorable toxicity profile. A microtubule-modulating anticancer agent, (S)-3-((R)-9-bromo-4-methoxy-6-methyl-5,6,7,8-tetrahydro-[1,3]dioxolo[4,5-g]isoquinolin-5-yl)-6,7-dimethoxyisobenzofuran-1(3H)-one (EM011) does not cause any hemo-, immuno-, and neuronal toxicity [23–25,27]. Since both docetaxel and EM011 bind at different sites on tubulin as per our *in silico* molecular docking predictive studies, we explored the synergism between these two drugs and investigated if induction of a well-tolerated drug could cause a reduction in the dose-regimen of the more toxic drug, docetaxel. Our data show that EM011 displays remarkable synergism with docetaxel that is widely used in the clinic today for prostate cancer therapy.

Another clinically relevant perspective that the present study supports is the sequence and timing of drug administration. Our dual-color cell-cycle data offers evidence to strengthen the emerging notion that induction of chronic mitotic arrest and prevention of mitotic exit is a favorable chemotherapeutic strategy [44]. Given the significant enhancement of mitotic population upon sequential treatment regimen that resulted in a synergistic

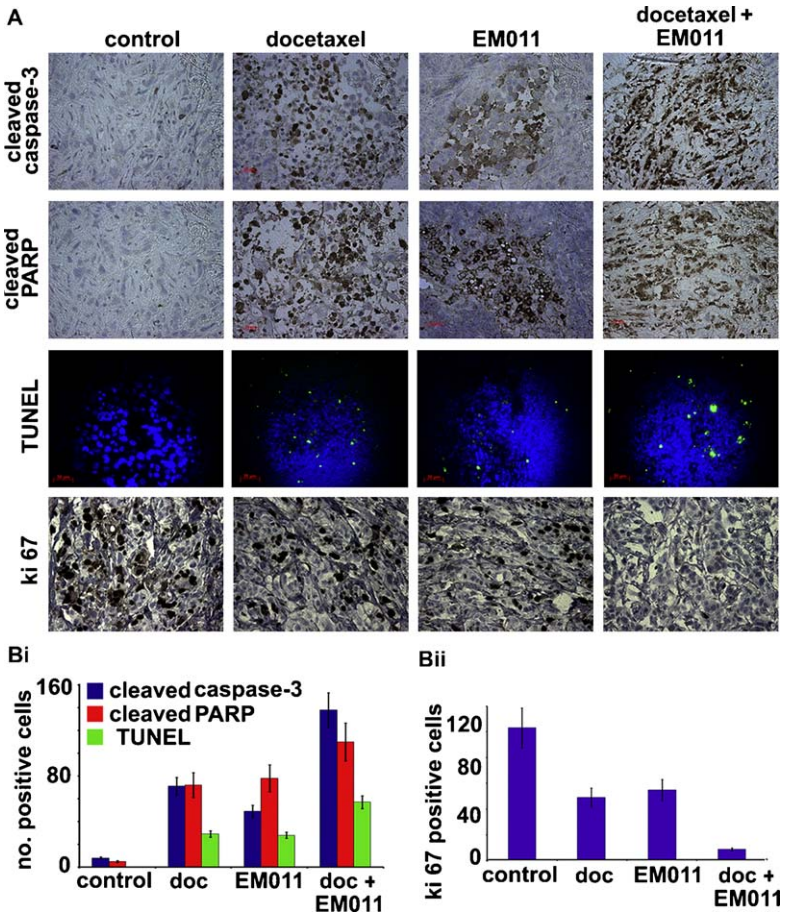

Fig. 6. (A) Immunohistochemical staining of tumor tissue sections from all treatment groups for apoptotic markers, cleaved caspase-3, cleaved PARP, TUNEL and proliferation marker, Ki67. (Bi and ii) Quantitation of immunohistochemical data (doc, docetaxel).

apoptotic population, it is reasonable to suggest that the durability and intensity of mitotic arrest has a strong bearing on the apoptotic index. Efforts to identify the key proapoptotic players that accumulate during the prolonged mitotic arrest are currently underway in our laboratory. The possibility that there might be an attenuation of antiapoptotic signals during the durable mitotic arrest is also plausible and is also currently under investigation.

In conclusion, our data for EM011-docetaxel combination presents a clinically relevant and a unique opportunity to reduce the dose-levels of docetaxel well below its maximum tolerated doses by compensating it with daily oral EM011 doses in prostate cancer therapy. Such approaches facilitating the use of lower dose-levels of more toxic-drugs can perhaps reduce toxicity to a significant extent, thus improving the quality of life of cancer patients.

Acknowledgement

This work was supported by grants to RA from Department of Defense and the National Cancer Institute (NIH).

Appendix A. Supplementary data

Supplementary data associated with this article can be found, in the online version, at doi:10.1016/j.bcp.2010.11.006.

References

[1] Lassi K, Dawson NA. Update on castrate-resistant prostate cancer: 2010. Curr Opin Oncol 2010;22:263–7.
[2] Loberg RD, Logothetis CJ, Keller ET, Pienta KJ. Pathogenesis and treatment of prostate cancer bone metastases: targeting the lethal phenotype. J Clin Oncol 2005;23:8232–41.
[3] Berthold DR, Sternberg CN, Tannock IF. Management of advanced prostate cancer after first-line chemotherapy. J Clin Oncol 2005;23:8247–52.
[4] Carroll PR, Kantoff PW, Balk SP, Brown MA, D'Amico AV, George DJ, et al. Overview consensus statement. Newer approaches to androgen deprivation therapy in prostate cancer. Urology 2002;60:1–6.
[5] Mazhar D, Waxman J. Early chemotherapy in prostate cancer. Nat Clin Pract Urol 2008;5:486–93.
[6] Wilkinson S, Chodak GW. Critical review of complementary therapies for prostate cancer. J Clin Oncol 2003;21:2199–210.
[7] Beer TM, Pierce WC, Lowe BA, Henner WD. Phase II study of weekly docetaxel in symptomatic androgen-independent prostate cancer. Ann Oncol 2001;12:1273–9.
[8] Petrylak DP. Chemotherapy for androgen-independent prostate cancer. World J Urol 2005;23:10–3.
[9] Aneja R, Asress S, Dhiman N, Awasthi A, Rida PCG, Arora SK, et al. Non-toxic melanoma therapy by a novel tubulin-binding agent. Int J Cancer 2010;126:256–65.
[10] Mancuso A, Oudard S, Sternberg CN. Effective chemotherapy for hormone-refractory prostate cancer (HRPC): present status and perspectives with taxane-based treatments. Crit Rev Oncol Hematol 2007;61:176–85.
[11] Moore CN, George DJ. Update in the management of patients with hormone-refractory prostate cancer. Curr Opin Urol 2005;15:157–62.
[12] Petrylak DP. Docetaxel for the treatment of hormone-refractory prostate cancer. Rev Urol 2003;5:S14–21.
[13] Quasthoff S, Hartung HP. Chemotherapy-induced peripheral neuropathy. J Neurol 2002;249:9–17.
[14] Rowinsky EK. The development and clinical utility of the taxane class of anti-microtubule chemotherapy agents. Annu Rev Med 1997;48:353–74.
[15] Jordan MA, Wilson L. Microtubules as a target for anticancer drugs. Nat Rev Cancer 2004;4:253–65.
[16] Clark EA, Hills PM, Davidson BS, Wender PA, Mooberry SL. Laulimalide and synthetic laulimalide analogues are synergistic with paclitaxel and 2-methoxyestradiol. Mol Pharm 2006;3:457–67.
[17] Honore S, Kamath K, Braguer D, Horwitz SB, Wilson L, Briand C, et al. Synergistic suppression of microtubule dynamics by discodermolide and paclitaxel in non-small cell lung carcinoma cells. Cancer Res 2004;64:4957–64.

[18] Wilmes A, Bargh K, Kelly C, Northcote PT, Miller JH, Peloruside. A synergizes with other microtubule stabilizing agents in cultured cancer cell lines. Mol Pharm 2007;4:269–80.
[19] Ye K, Ke Y, Keshava N, Shanks J, Kapp JA, Tekmal RR, et al. Opium alkaloid noscapine is an antitumor agent that arrests metaphase and induces apoptosis in dividing cells. Proc Natl Acad Sci U S A 1998;95:1601–6.
[20] Aneja R, Lopus M, Zhou J, Vangapandu SN, Ghaleb A, Yao J, et al. Rational design of the microtubule-targeting anti-breast cancer drug EM015. Cancer Res 2006;66:3782–91.
[21] Aneja R, Vangapandu SN, Lopus M, Chandra R, Panda D, Joshi HC. Development of a novel nitro-derivative of noscapine for the potential treatment of drug-resistant ovarian cancer and T-cell lymphoma. Mol Pharmacol 2006;69:1801–9.
[22] Aneja R, Vangapandu SN, Lopus M, Viswesarappa VG, Dhiman N, Verma A, et al. Synthesis of microtubule-interfering halogenated noscapine analogs that perturb mitosis in cancer cells followed by cell death. Biochem Pharmacol 2006;72:415–26.
[23] Aneja R, Zhou J, Vangapandu SN, Zhou B, Chandra R, Joshi HC. Drug-resistant T-lymphoid tumors undergo apoptosis selectively in response to an anti-microtubule agent, EM011. Blood 2006;107:2486–92.
[24] Aneja R, Liu M, Yates C, Gao J, Dong X, Zhou B, et al. Multidrug resistance-associated protein-overexpressing teniposide-resistant human lymphomas undergo apoptosis by a tubulin-binding agent. Cancer Res 2008;68:1495–503.
[25] Aneja R, Zhou J, Zhou B, Chandra R, Joshi HC. Treatment of hormone-refractory breast cancer: apoptosis and regression of human tumors implanted in mice. Mol Cancer Ther 2006;5:2366–77.
[26] Chou TC, Talalay P. Quantitative analysis of dose-effect relationships: the combined effects of multiple drugs or enzyme inhibitors. Adv Enzyme Regul 1984;22:27–55.
[27] Aneja R, Miyagi T, Karna P, Ezell T, Shukla D, Vij Gupta M, et al. A novel microtubule-modulating agent induces mitochondrially driven caspase-dependent apoptosis via mitotic checkpoint activation in human prostate cancer cells. Eur J Cancer 2010;46:194–204.
[28] Karna P, Sharp SM, Yates C, Prakash S, Aneja R. EM011 activates a survivin-dependent apoptotic program in human non-small cell lung cancer cells. Mol Cancer 2009;8:93.
[29] Kavallaris M. Microtubules and resistance to tubulin-binding agents. Nat Rev Cancer 2010;10:194–204.
[30] Ravelli RB, Gigant B, Curmi PA, Jourdain I, Lachkar S, Sobel A, et al. Insight into tubulin regulation from a complex with colchicine and a stathmin-like domain. Nature 2004;428:198–202.
[31] Dixon SL, Smondyrev AM, Knoll EH, Rao SN, Shaw DE, Friesner RA. PHASE: a new engine for pharmacophore perception, 3D QSAR model development, and 3D database screening: 1. methodology and preliminary results. J Comput Aided Mol Des 2006;20:647–71.
[32] Dixon WE, Malden W. Colchicine with special reference to its mode of action and effect on bone-marrow. J Physiol 1908;37:50–76.
[33] Meng EC, Pettersen EF, Couch GS, Huang CC, Ferrin TE. Tools for integrated sequence-structure analysis with UCSF Chimera. BMC Bioinformatics 2006;7:339.
[34] Pettersen EF, Goddard TD, Huang CC, Couch GS, Greenblatt DM, Meng EC, et al. UCSF Chimera—a visualization system for exploratory research and analysis. J Comput Chem 2004;25:1605–12.
[35] Lowe J, Li H, Downing KH, Nogales E. Refined structure of alpha beta-tubulin at 3.5 A resolution. J Mol Biol 2001;313:1045–57.
[36] Aneja R, Kalia V, Ahmed R, Joshi HC. Nonimmunosuppressive chemotherapy: EM011-treated mice mount normal T-cell responses to an acute lymphocytic choriomeningitis virus infection. Mol Cancer Ther 2007;6:2891–9.
[37] Stewart ZA, Leach SD. Pietenpol JA. p21(Waf1/Cip1) inhibition of cyclin E/Cdk2 activity prevents endoreduplication after mitotic spindle disruption. Mol Cell Biol 1999;19:205–15.
[38] Stewart ZA, Mays D, Pietenpol JA. Defective G1-S cell cycle checkpoint function sensitizes cells to microtubule inhibitor-induced apoptosis. Cancer Res 1999;59:3831–7.
[39] Vaziri C, Saxena S, Jeon Y, Lee C, Murata K, Machida Y, et al. A p53-dependent checkpoint pathway prevents rereplication. Mol Cell 2003;11:997–1008.
[40] Rubin SJ, Hallahan DE, Ashman CR, Brachman DG, Beckett MA, Virudachalam S, et al. Two prostate carcinoma cell lines demonstrate abnormalities in tumor suppressor genes. J Surg Oncol 1991;46:31–6.
[41] Shi J, Orth JD, Mitchison T. Cell type variation in responses to antimitotic drugs that target microtubules and kinesin-5. Cancer Res 2008;68:3269–76.
[42] Huang HC, Shi J, Orth JD, Mitchison TJ. Evidence that mitotic exit is a better cancer therapeutic target than spindle assembly. Cancer Cell 2009;16:347–58.
[43] Gascoigne KE, Taylor SS. Cancer cells display profound intra- and interline variation following prolonged exposure to antimitotic drugs. Cancer Cell 2008;14:111–22.
[44] Weaver BA, Cleveland DW. Decoding the links between mitosis, cancer, and chemotherapy: the mitotic checkpoint, adaptation, and cell death. Cancer Cell 2005;8:7–12.
[45] Hsieh CL, Xie Z, Liu ZY, Green JE, Martin WD, Datta MW, et al. A luciferase transgenic mouse model: visualization of prostate development and its androgen responsiveness in live animals. J Mol Endocrinol 2005;35:293–304.
[46] Petrylak DP. The treatment of hormone-refractory prostate cancer: docetaxel and beyond. Rev Urol 2006;8:S48–55.